J. Physiol. (1984), **354**, *pp.* 445–456
With 2 plates and 1 text-figure
Printed in Great Britain

EXCHANGE AREA AND SURFACE PROPERTIES OF THE MICROVASCULATURE OF THE RABBIT SUBMANDIBULAR GLAND FOLLOWING DUCT LIGATION

BY GERALDINE CLOUGH* AND L. H. SMAJE

*From the * University Laboratory of Physiology, Oxford OX1 3PT and Department of Physiology, Charing Cross and Westminster Medical School, Fulham Palace Road, London W6 8RF*

(*Received 1 March 1984*)

SUMMARY

1. The exchange area of the submandibular salivary gland microvasculature has been measured to allow the value of microvascular permeability (P) to hydrophilic solutes to be calculated from previous measurements of permeability–surface area (PS) products.

2. Glands whose ducts had been ligated for 2 weeks and the contralateral control glands were perfusion-fixed with a modified Karnovsky's fixative after perfusion with a solution containing cationized ferritin, and examined with transmission electron microscopy.

3. Stereological techniques were used to estimate the surface area of the exchange vessels on random thin sections from four control and four duct-ligated glands. The mean exchange surface area in control glands was 512 $cm^2 g^{-1}$ and 336 $cm^2 g^{-1}$ in duct-ligated glands. The fenestral density was calculated to be 0·57 % of the exchange surface in control glands and 0·30 % in duct-ligated tissue.

4. Molecules of cationized ferritin appeared bound to the luminal surface of the microvascular endothelium, including the surface of the fenestrae to a depth of about 25 nm in both control and ligated glands.

5. These experiments have shown that the exchange surface area of the fenestrated endothelium of the submandibular salivary gland is comparable to that in cardiac muscle but the permeability (P) to small solutes is about 10 times greater. Following ligation of the salivary gland duct, solute permeability falls and an explanation of this, based on the reduced surface area and the nature of the permeability–flow relationship for small solutes is offered.

INTRODUCTION

The microvasculature of the submandibular salivary gland has been shown to be very permeable to small hydrophilic solutes (Mann, Smaje & Yudilevich, 1979*a*). This permeability, measured as a permeability–surface area product (PS) (Martin de Julian & Yudilevich, 1964) is much higher than that of other non-fenestrated vascular beds. In order to provide quantitative estimates of permeability (P) from the

PS data, the total surface area (*S*) of the exchange microvasculature must be known. Information concerning the fenestral density is also important as the high permeability in fenestrated capillaries is generally assumed to be a consequence of the presence of the fenestrae.

Ligation of the main duct of the salivary gland for 2 weeks leads to a fall in *PS* product to Cr EDTA, vitamin B_{12} and insulin (Mann, Smaje & Yudilevich, 1979*b*). The fall in *PS* product, however, cannot be attributed for certain to a change in either *P* or *S*. In this situation neither *S* nor *P* may be controlled, and both are unknown. In order to investigate these problems, a quantitative survey of the normal and duct-ligated salivary gland microvasculature has been made, together with estimates of the exchange surface area and fenestral density.

There is increasing evidence that the permeability properties of the walls of continuous capillaries are at least in part determined by the cell coat or glycocalyx shown to line the capillary endothelium (Luft, 1966; Shirahama & Cohen, 1972; Michel, 1981). Such a cell coat has also been shown to line the fenestrated capillaries of the pancreas (Simionescu & Simionescu, 1981) and it is possible that such a cell coat could help to explain the permeability properties of fenestrated capillaries.

In order to determine the nature of the surface coat lining the endothelium of the fenestrated capillaries of the salivary gland and to investigate possible changes in this coat following duct ligation, the binding of a macromolecule known to delineate the cell surface coat, cationized ferritin (Simionescu & Simionescu, 1981; Turner, Clough & Michel, 1983) has been quantitatively estimated in the microcirculation of both control and duct-ligated glands.

Some of the findings presented here have been described in abstract previously (Clough & Smaje, 1984; Smaje, 1983).

METHODS

Chronic duct ligation

Four New Zealand White rabbits weighing between 2·5 and 3·5 kg were anaesthetized with halothane gas and their necks shaved. Following a right paramedian incision, the mylohyoid muscle was split and the right submandibular duct exposed and ligated rostral to the point where it is joined by the chorda tympani nerve, in order to preserve the nerve. The subcutaneous tissue and skin were sutured and recovery was uneventful in all cases. Full aseptic precautions were used throughout.

Gland perfusion and fixation

Two weeks after the initial duct ligation the animals were anaesthetized with urethane (1·8 g kg^{-1}, I.V.) and prepared for surgery. Anaesthesia was supplemented as required via a cannula in the femoral vein. The right submandibular salivary gland and its vasculature was exposed together with that of the left (control) gland. The external maxillary artery was exposed as it crossed the mandible and cannulated in a retrograde direction until the cannula tip was just distal to the junction of the submandibular artery. Perfusion with warmed, oxygenated Krebs solution was then started and the external maxillary artery was ligated proximal to the submandibular artery, thereby isolating the gland. The gland was perfused at a pressure of 20–30 cmH_2O until the venous effluent was free of blood, at which point the perfusate was switched to one containing 0·1 g cationized ferritin in 100 ml Krebs solution, 5 ml of which was delivered to each gland in 1 min, using a constant infusion pump. Free cationized ferritin was then washed from the circulation by re-perfusion with Krebs solution and both glands were fixed by perfusion with a modified Karnovsky's fixative.

The Krebs solution used had the following composition in mmol l^{-1}: NaCl, 118; KCl, 4·7; KH_2PO_4, 1·1; $MgSO_4.7H_2O$, 1·25; $NaHCO_3$, 25; $CaCl_2$, 2·5; and D-glucose, 11·1. It was bubbled with 95% O_2,/5% CO_2 and had a pH of 7·4.

Cationized ferritin was either purchased from Sigma Chemical Co. Ltd. at a concentration of 100 mg ml^{-1} in 0·9% NaCl with an estimated isoelectric point (pI) of 8·4, or it was made from native ferritin (Sigma) using the method of Danon, Goldstein, Marikovsky & Skutelsky (1972) as described by Turner *et al.* (1983) to give a polycationic ferritin with a pI of greater than 10·5. Both cationized ferritin solutions were diluted with Krebs solution to give a final concentration of 0·1 g cationized ferritin in 100 ml Krebs solution.

Preparation for electron microscopy

The glands were removed from the animal, cut into 0·5 mm blocks and immersed in fixative for a further 12–24 h. The tissue was post-fixed in 2% osmium tetroxide and prepared for transmission electron microscopy. Thin (50 nm) sections were cut from random blocks of tissue and mounted on uncoated copper grids. They were stained with uranyl acetate and lead citrate and examined in a Jeol 100CX transmission electron microscope at an accelerating voltage of 60 kV.

Estimates of exchange surface area

The vessels included in the estimates of exchange surface area were of internal diameter less than 20 μm with no smooth muscle in their walls.

Two methods of estimating exchange surface area were used:

(a) Direct capillary counting, in which the number of capillaries per unit area of tissue was estimated from areas of each section of the gland, selected at random and viewed directly through the microscope. The diameters of the microvessels were measured on low-power electron micrographs (×4200) of the same areas.

(b) Stereological intercept counting, in which an interrupted grid which consisted of eighty-four short lines of total length 100·8 cm was placed over random low power (×4200) electron micrographs of the gland tissue and the number of intercepts between the grid lines and the walls of the exchange vessels was counted. A measure of the exchange surface density (S_v) was obtained from the relationship described by Weibel (1979) in which,

$$S_v = 2.\Sigma I_c/\Sigma L_{total}\ cm^{-1},$$

where ΣI_c is the total number of intercepts of the walls of microvessels with grid lines, ΣL_{total} is the total length of grid lines superimposed on the gland tissue corrected for magnification of the micrographs.

Endothelial morphology

(a) Fenestral density and structure were investigated using low-power electron micrographs (×4200) of random areas of the gland.

(b) The binding of cationized ferritin molecules to the surface coat was investigated using high-power electron micrographs (×87000) of the microvascular endothelium, from which counts of the number of cationized ferritin molecules adjacent to the cell surface could be made.

All values quoted are the mean ± 1 S.E. of mean, and where statistical comparisons have been made Student's *t* test was used.

RESULTS

Exchange surface area of the gland microcirculation

Values for the exchange surface area of the healthy and duct-ligated gland microcirculation were obtained by (a) estimating microvascular density and (b) stereological intercept counting.

(*a*) *Direct estimates of exchange vessel density.* Estimates of the numbers of exchange vessels per unit area of gland tissue examined under low-power electron microscopy showed there to be significantly fewer vessels ($P < 0·001$) in the ligated tissue than in the control healthy tissue. In 123 sections of healthy tissue from four rabbits the

number of vessels per square centimetre was $142{\cdot}0 \times 10^3 \pm 5{\cdot}4 \times 10^3$, and in eighty-seven sections of duct-ligated tissue from the same four rabbits, the number was $48{\cdot}4 \times 10^3 \pm 12{\cdot}3 \times 10^3$ vessels cm^{-2}.

The mean diameter of these vessels was estimated by making measurements of the smallest internal diameter of each vessel on ×4200 electron micrographs. The

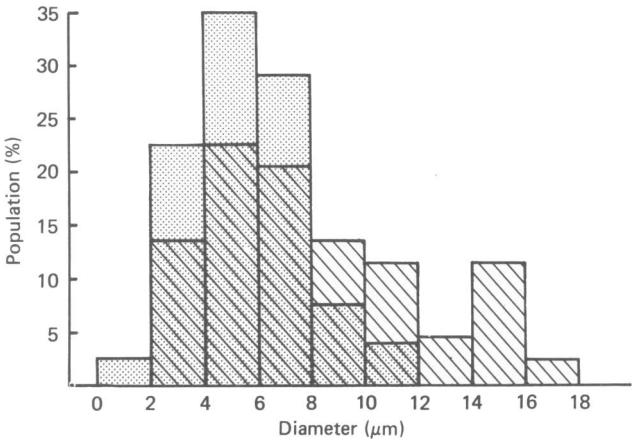

Fig. 1. Distribution of the minimum internal diameters of microvessels, up to 20 μm diameter, in control (stippled bars) and duct-ligated (hatched bars) submandibular salivary glands. Ordinate values are expressed as a percentage of the total number of vessels measured (eighty-four in control glands and forty-three in duct-ligated glands). Measurements were made on ×4200 electron micrographs.

smallest diameter was measured to avoid over-estimation of the diameter by measuring vessels sectioned obliquely. In control tissue the diameter was $5{\cdot}94 \pm 0{\cdot}32$ μm ($n = 84$), which was significantly lower than that of vessels from duct-ligated tissue which was $7{\cdot}79 \pm 0{\cdot}59$ μm ($n = 43$) (see Table 1). Fig. 1 shows the distribution of vessel diameters from control and duct-ligated glands. It demonstrates that the mode of the two populations is similar, the increase in mean diameter following duct ligation being due to the appearance of a few larger vessels. The total surface area of vascular endothelium of the exchange vessels per gram of tissue was calculated to be 267 $cm^2\ g^{-1}$ in the control tissue and 119 $cm^2\ g^{-1}$ in the duct-ligated tissue, if the mean values of vessel diameter are used and if vessels are assumed to be aligned in parallel.

(*b*) *Intercept counting.* The grid counting method of Weibel (1979) described in the Methods section was used to estimate the surface density of the exchange area of the microvascular bed per unit volume of gland from four control glands and four duct-ligated glands. The mean values were $511{\cdot}9 \pm 53{\cdot}9$ cm^{-1} ($n = 30$) in control tissue and $336{\cdot}1 \pm 46{\cdot}7$ cm^{-1} ($n = 29$) in duct-ligated tissue, which were significantly different at the $P < 0{\cdot}001$ level (Table 1).

The course of the microvessels through the tissue is dictated by the acinar structure, i.e. they are more or less randomly orientated. Whilst the method described by Weibel (1979) allows for this and is independent of the degree of capillary orientation if truly random sections of the gland are taken, the direct calculation of

surface area in Method (a) does not. In this calculation vessels are falsely assumed to run perpendicular to the section face. Weibel (1979) has shown that allowance for this can be made by correcting the calculated value of surface area by a factor $c(k)$ which will have a value of 2 if the capillaries are truly random and 1 if they are completely aligned.

TABLE 1. Summary of morphometric data obtained from four ligated and four contralateral control rabbit submandibular salivary glands. See text for details

	Salivary gland	
	Control	Ligated
Capillaries		
Total area ($cm^2\ g^{-1}$)	512 ± 54	336 ± 47
Diameter (μm)	$5{\cdot}94 \pm 0{\cdot}32$	$7{\cdot}79 \pm 0{\cdot}59$
Fenestrae		
No. per profile	$2{\cdot}57 \pm 0{\cdot}54$	$1{\cdot}80 \pm 0{\cdot}67$
Diameter (nm)	$53{\cdot}2 \pm 1{\cdot}9$	$52{\cdot}6 \pm 1{\cdot}6$
Area per unit area capillary	$5{\cdot}75 \times 10^{-3}$	$3{\cdot}03 \times 10^{-3}$
Area per mass of gland ($cm^2\ g^{-1}$)	2·9	1·0

If complete randomness is assumed and the calculated values of surface area are corrected by a factor of 2, to become 534 $cm^2\ g^{-1}$ for control tissue and 238 $cm^2\ g^{-1}$ for duct-ligated tissue, they more closely approximate to values estimated by using the intercept counting method (512 and 336 $cm^2\ g^{-1}$, respectively).

Exchange surface morphology

(*a*) *General gland morphology.* Examination of the healthy salivary gland with both light microscopy and low-power electron microscopy showed the lobules of the gland to comprise relatively tightly packed areas of acinar tissue and its vasculature, with little interstitial material separating the acinar regions. The ducts draining the acinar tissue were well formed with regularly shaped lumina.

Following 2 weeks of duct ligation, the submandibular salivary gland appeared oedematous, with irregularly shaped areas of acinar tissue separated by large areas of fibrous connective tissue. The vascular endothelium also appeared oedematous and the small vessels were frequently irregular in shape and appearance. The ducts were much enlarged and their lumina grossly distorted (see Pl. 1).

(*b*) *Distribution of fenestrae.* The number of fenestrae (both with and without diaphragms) within each vessel profile was also counted from low-power electron micrographs. Estimates of the mean number of fenestrae per vessel profile showed there to be no significant change following duct ligation. In control tissue the number was $2{\cdot}57 \pm 0{\cdot}72$ fenestrae per profile ($n = 123$) compared with $1{\cdot}80 \pm 0{\cdot}67$ fenestrae per profile ($n = 87$) in ligated tissue. Measurement of the diameter of forty-one fenestrae, twenty-three from control vessels and eighteen from duct-ligated vessels all covered by a diaphragm, showed there to be no significant change in diameter following duct ligation (see Table 1). Together they yielded a mean value for fenestral diameter of

52·7 ± 1·2 nm. These values give a fenestral density of 0·57 % and 0·30 % of microvascular surface area for control and ligated gland tissue, respectively. They are maximal values as they do not take into account possible over-estimates of fenestral numbers due to sectioning artifacts.

An attempt was made to distinguish between exchange vessels associated with acinar tissue and those lying close to salivary ducts. As the majority of vessels photographed (83 % of control vessels and 90 % of duct-ligated vessels) were associated with acinar tissue little significance could be placed on these results. They did suggest however that duct ligation results in a small decrease in the number of capillaries associated with acinar tissue and that these vessels had fewer fenestrae per vessel profile (1·47 ± 1·08, $n = 78$) than vessels from control tissue (3·44 ± 1·85, $n = 101$).

(c) *Distribution of cationized ferritin in the vasculature of the control and duct-ligated glands.* The binding of molecules of cationized ferritin to the luminal surface of the endothelium of the walls of the gland microvasculature was found to be somewhat variable, and partly dependent on how well the vasculature had been washed free of blood prior to perfusion with the cationized ferritin solution, and partly on the type of cationized ferritin used. The commercial cationized ferritin, which had a lower pI (8·4) than that made in the laboratory (pI > 10·5) appeared to bind less well to the endothelial cell surface of the control gland tissue (Pl. 2*A* and *B*). It did however bind to the diaphragms which covered the fenestrae, and gave a picture reminiscent of that published by Simionescu & Simionescu (1981) in the intestine and pancreas.

The problems of staining and sectioning did not allow the presence or absence of diaphragms from fenestrae to be carefully analysed, and in the present study no further detail can be given.

When the commercially made ferritin was used, few of the necks of the vesicles open to the luminal endothelial cell surface were covered by molecules of cationized ferritin. In addition none of the vesicles contained molecules of ferritin. The more highly cationized ferritin made in the laboratory did appear to cover the majority of the mouths of the luminal vesicles, but less than 1 % of these vesicles appeared labelled with molecules of ferritin. This finding is in direct contrast with the observation that the majority of the vesicles from the endothelium of continuous capillaries of the frog mesentery label with molecules of cationized ferritin under similar conditions (Clough, 1982).

Plate 2*B* shows molecules of the more highly cationized ferritin binding in a continuous layer covering the whole of the luminal surface of the endothelium, including the vesicle necks, the fenestral diaphragms, and even the gaps of open fenestrae where it appears to reach but not pass through the basement membrane. Repeated measurements of the thickness of this layer of cationized ferritin molecules on nineteen random high-power electron micrographs give a thickness of 25·6 ± 1·5 nm, a value very close to that reported by Clough (1982) and Turner *et al.* (1983) in the continuous capillaries of the frog mesentery. This does suggest that a cell coat is present at the surface of fenestrated endothelium and that it has similar binding properties to that of the continuous capillaries.

Molecules of cationized ferritin were also seen to bind to the endothelial cell surface of vessels from duct-ligated glands (Pl. 2*C*). The depth of this layer was however very variable, and large aggregates of molecules of cationized ferritin were often

seen within the vessel lumen or closely associated with the endothelial cell wall (Pls. 1 and 2*C*).

In one animal in which the layer of cationized ferritin molecules was more regular in both the control gland vasculature and that of the duct-ligated gland, estimates of the concentration of molecules of cationized ferritin within the layer were made from micrographs. The mean concentration of cationized ferritin within the layer in seven capillaries from each gland was $5{\cdot}9 \pm 0{\cdot}06 \times 10^4$ molecules μm^{-3} in control tissue and $4{\cdot}4 \pm 0{\cdot}07 \times 10^4$ molecules μm^{-3} in ligated tissue, if a section thickness of 50 nm is assumed. These estimates of the concentration of cationized ferritin molecules in the layer are very close to those previously reported in that covering the endothelium of the continuous capillaries of the frog mesentery (Clough, 1982; Turner *et al.* 1983).

DISCUSSION

The aim of the experiments described in this paper was to obtain a quantitative estimate of the exchange surface area of the fenestrated endothelium of the microvasculature of the submandibular salivary gland and to estimate the density of fenestrae within this area. The effects of chronic ligation of the submandibular salivary duct on the exchange surface were also investigated. The values of surface area (*S*) obtained allow permeability (*P*) to be calculated from previously published values of permeability–surface area products (*PS*) for small solutes in the salivary gland (Mann *et al.* 1979*a*, *b*) and permit these values of permeability for the fenestrated endothelium of the salivary gland to be compared with values of permeability for continuous endothelium.

Estimates of surface area in the control gland

Previous attempts to estimate the vascular exchange surface area of the submandibular salivary gland by the use of Indian ink injection and immersion fixation have yielded values of between 380 and 420 $cm^2\ g^{-1}$ if a parallel array of capillaries is assumed (Buran & Smaje, 1982; Smaje & Olive, see Smaje, 1983). The present estimates obtained from perfusion-fixed tissue using low-power electron microscopy are somewhat lower when similar assumptions about capillary arrangement are made, probably reflecting the problem of specimen shrinkage during immersion fixation. The higher value of exchange surface area obtained by intercept counting is a closer estimate of the true surface area as the technique does not assume a homogeneity of vascular arrangement.

Table 2 illustrates the variation in surface area in both continuous and fenestrated capillaries. It is interesting to note that the salivary gland, cardiac muscle and intestinal mucosa have comparable capillary densities which must surely reflect their metabolic activity. The intestinal mucosa for example has a capillary surface area about 4 times that of the muscularis (Casley-Smith, O'Donoghue & Crocker, 1975) and receives a comparably greater blood flow (Lundgren, 1967; Granger, Richardson & Taylor, 1979).

Estimates of permeability of the normal salivary gland

If the value for surface area is taken to be 512 $cm^2\ g^{-1}$, it is possible to calculate values for the permeability (*P*) of the gland for a range of molecules using the *PS*

data of Mann *et al.* (1979*a*, *b*). These data were obtained from the cat submandibular gland, and whilst it is probably not wholly desirable that data from the rabbit and cat should be combined, as yet there are insufficient data from one species to allow comparison. The values of P obtained may be compared with those of other vascular

TABLE 2. Comparison of capillary permeability and filtration coefficients in the salivary gland with those in other vascular beds

	Salivary gland	Interstitial mucosa	Cardiac muscle	Skeletal muscle
K_f (ml min^{-1} 100 g^{-1} mmHg^{-1})	1·3[a]	0·7*[b]	0·34[c]	0·014[c]
PS (ml min^{-1} 100 g^{-1})				
Sucrose or EDTA	800[d]	136*[e]	56[e]	4·3[e]
Inulin	176[d]	68*[e]	13[e]	1·0[e]
Albumin	0·13[f]	0·091†[g]	0·097[h]	0·004[c]
Surface area (cm^2 g^{-1})	512[k]	276[i]	500[j]	70[c]
Fenestral density (cm^2 g^{-1})	2·94[k]	1·58[i]		
L_p (cm^3 s^{-1} dyn^{-1} × 10^{10})	3·1	3·2*	0·86	0·25
P (cm s^{-1} × 10^6)				
Sucrose or Cr EDTA	270	82*	17	10
Inulin	57	41*	4·3	2·3
Albumin	0·04	0·12†	0·03	0·01
K_f/PS inulin × 10^3	7·4	10	26	14

References to the values quoted are as follows: (a) J. Gamble, L. H. Smaje & P. D. Spencer (unpublished), (b) Granger *et al.* (1979), (c) Renkin, & Curry (1978), (d) Mann *et al.* (1979*a*), (e) Crone (1984), (f) Koo, Smaje & Spencer (1981), (g) Granger & Taylor (1980), (h) Renkin (1977), (i) Casley-Smith *et al.* (1975), (j) Basingthwaighte, Yipintsoi & Harvey (1974), (k) present paper.

* Calculated from values for the whole intestine assuming the mucosa comprises 28 % of intestinal weight (Casley-Smith *et al.* 1975) and that the muscularis has K_f and PS values indentical to those in skeletal muscle.

† Value for whole intestine. P albumin calculated on basis of whole intestine surface area of 125 cm^2 g^{-1} (Casley-Smith *et al.* 1975).

beds for a range of solutes (Table 2). It is gratifying to note that when total and fenestral surface area are taken into account, the two fenestrated beds have fairly similar hydraulic conductivities, L_p and P values. The higher capillary filtration coefficients, K_f and PS in cardiac muscle compared with skeletal muscle are not reflected in comparably greater L_p and P when surface area is taken into account, but this procedure does serve to emphasize the difference between the continuous and fenestrated capillary types. If this difference were a consequence of a greater mean size of the channels through which water and solute are moving in fenestrated capillaries, then one would expect K_f to be increased more than PS. In the event, the ratio K_f/PS is similar for all types of capillaries, suggesting that the presence of the fenestrae increases exchange by increasing the area and by reducing the path length. The present finding that cationized ferritin binds to a layer 25 nm thick which covers the whole of the endothelial cell surface, including the fenestrae, suggests that a cell coat or glycocalyx may well be responsible for the sieving characteristics of these capillaries. It must not be forgotten, however, that other structures such as the basement membrane of the interstitium may also play a role in limiting exchange across the fenestrated endothelium of the gland, particularly as calculated diffusional

exchange across the fenestrae is much greater than that actually observed (Casley-Smith *et al.* 1975; Smaje, 1983).

Estimates of surface area in the duct-ligated salivary gland

Ligation of the submandibular salivary duct appears to cause a reduction of about 35 % in the exchange surface area of the gland vascular bed. This reduction occurs chiefly as a result of a dramatic decrease in the number of exchange vessels within

TABLE 3. Data from Mann *et al.* (1979*b*) showing the effect of duct ligation on *PS* values. Predicted values were determined from the *PS* expected from the *PS vs.* flow relationship (Mann *et al.* 1979*a*) × ratio ligated area : control area for total capillary surface area and fenestral area respectively. See text for further details

	Control *PS* ($cm^2\ g^{-1}$)	Ligated *PS* ($cm^2\ g^{-1}$)		
		Predicted		Observed
		From fall in total surface area	From fall in fenestral area	
Cr EDTA	5·26	6·55	3·45	4·20
B_{12}	3·22	2·6	1·4	2·02
Insulin	1·52	1·3	0·68	0·72

the gland, but is somewhat masked by the fact that the diameter of the remaining vessels appears to increase. There may also be a small reduction in the number of fenestrae per vessel profile, which becomes significant when the total fenestral area is calculated. Following duct ligation the fenestral area falls from 0·6 % of the vascular surface to occupy only 0·3 % of the total exchange surface.

Estimates of permeability of the duct-ligated salivary gland

The data obtained for the exchange surface area in the present experiments may be used to calculate values of *P* from *PS* values obtained by Mann *et al.* (1979*b*). As can be seen from Table 1, the ratio ligated gland : control gland surface area is 0·66 and that for fenestral area is 0·34. This must explain, in part, the fall in *PS*, but the differential fall apparent for the different solutes requires further consideration.

One possible explanation for this may lie in the fact that *PS* for Cr EDTA was flow limited even at the highest flows used, while B_{12} became diffusion limited only over 8 ml $min^{-1}\ g^{-1}$ (Mann *et al.* 1979*a*). Inulin and insulin were essentially diffusion limited at all flows over 5 ml $min^{-1}\ g^{-1}$. Since total flow remains constant, each of the reduced number of capillaries would have had a flow about 1·7 times that in the control gland.

If, in the duct-ligated glands, Cr EDTA were still flow limited, or just becoming diffusion limited as seems likely, the increased individual capillary flow would lead to an increased individual capillary *PS* and the effect of the reduced surface area would be minimized. A fall in *PS* smaller than the fall in surface area would be predicted. With vitamin B_{12}, diffusion-limited exchange would be expected at a lower flow than in the control gland, and this is what is found. *PS* was independent of flow at flows above 4 ml $min^{-1}\ g^{-1}$ (Mann *et al.* 1979*a*, *b*) and the fall in *PS* would be

expected to be in proportion to the fall in surface area, which it was. In the control gland *PS* for insulin was independent of flow at all flows over 5 ml min^{-1} g^{-1}, and the fall in *PS* for insulin would also be expected to be in proportion to that of the surface area. Table 3 shows the *PS* values found in the control and duct-ligated glands together with predicted values of *PS* following ligation. The *PS vs.* flow relationships measured by Mann *et al.* (1979*a*) were used to determine the *PS* expected at the increased flow, which was then multiplied by the ratio of capillary surface area or fenestral area following ligation to those of the control.

Since *PS* changes approximated those expected, as discussed above, it appears unlikely that there was also a change in the nature of the surface coat. The apparently uneven cationized ferritin binding following duct ligation in two of the ligated glands was most likely due to insufficient wash-out of blood. This interpretation gains credence from the presence of red blood cells in these capillaries (Pl. 1).

We would like to thank Miss Mary Olive and Mrs Ingrid White for their excellent technical assistance. The MRC are gratefully acknowledged for a grant for the purchase of the electron microscope, and for a project grant to L.H.S.

REFERENCES

BASSINGTHWAIGHTE, J. B., YIPINTSOI, T. & HARVEY, R. B. (1974). Microvasculature of the dog left ventricular myocardium. *Microvascular Research* **7**, 229–249.

BURAN, J. & SMAJE, L. H. (1982). The surface area of capillaries in the rabbit submandibular salivary gland. *Microvascular Research* **24**, 238.

CASLEY-SMITH, J. R., O'DONOGHUE, P. J. & CROCKER, K. W. J. (1975). The quantitative relationship between fenestrae in jejunal capillaries and connective tissue channels: proof of 'tunnel-capillaries'. *Microvascular Research* **9**, 78–100.

CLOUGH, GERALDINE (1982). The steady-state transport of cationized ferritin by endothelial cell vesicles. *Journal of Physiology* **328**, 389–401.

CLOUGH, GERALDINE & SMAJE, L. H. (1984). Changes in capillary morphology following chronic duct ligation of the rabbit submandibular gland. *Microvascular Research* **27**, 395–396.

CRONE, C. (1984). The function of capillaries. In *Recent Advances in Physiology*, ed. BAKER, P. F., pp. 125–162. Edinburgh: Churchill Livingstone.

DANON, D., GOLDSTEIN, L., MARIKOVSKY, Y. & SKUTELSKY, E. (1972). Use of cationized ferritin as a label of negative charges on cell surfaces. *Journal of Ultrastructural Research* **38**, 500–510.

GRANGER, D. N., RICHARDSON, P. D. I. & TAYLOR, A. E. (1979). Volumetric assessment of the capillary filtration coefficient in cat small intestine. *Pflügers Archiv* **381**, 25–33.

GRANGER, D. N. & TAYLOR, A. E. (1980). Permeability of intestinal capillaries to endogenous macromolecules. *American Journal of Physiology* **238**, H457–464.

KOO, A., SMAJE, L. H. & SPENCER, P. D. (1981). Low permeability to macromolecules of the fenestrated capillaries in the cat submandibular salivary gland. *Bibliotheca Anatomica* **20**, 301–304.

LUFT, J. H. (1966). Fine structure of capillary and endocapillary layer as revealed by ruthenium red. *Federation Proceedings* **25**, 1773–1783.

LUNDGREN, O. (1967). Studies on blood flow distribution and counter current exchange in the small intestine. *Acta physiologica scandinavica* **303**, suppl., 5–42.

MANN, G. E., SMAJE, L. H. & YUDILEVICH, D. L. (1979*a*). Permeability of the fenestrated capillaries in the cat submandibular gland to lipid-insoluble molecules. *Journal of Physiology* **297**, 335–354.

MANN, G. E., SMAJE, L. H. & YUDILEVICH, D. L. (1979*b*). Transcapillary exchange in the cat salivary gland during secretion, bradykinin infusion and after chronic duct ligation. *Journal of Physiology* **297**, 355–367.

MARTIN DE JULIAN, P. & YUDILEVICH, D. L. (1964). A theory for the quantification of transcapillary exchange by tracer dilution curves. *American Journal of Physiology* **207**, 162–168.

MICHEL, C. C. (1981). The flow of water through the capillary wall. In *Water Transport across Epithelia, Alfred Benzon Symposium 15*, ed. USSING, H. H., BRINDSLEV, N., LASSEN, N. A. & STEN-KNUDSEN, O., pp. 268–279. Copenhagen: Munksgaard.

RENKIN, E. M. (1977). Multiple pathways of capillary permeability. *Circulation Research* **41**, 735–743.

RENKIN, E. M. & CURRY, F. E. (1978). Transport of water and solutes across capillary endothelium. *Membrane Transport in Biology*, vol. IV A, *Transport Organs*, ed. GIEBISCH, G., TOSTESON, D. C. & USSING, H. H., pp. 1–45. Berlin, New York: Springer-Verlag.

SHIRAHAMA, T. & COHEN, A. S. (1972). The role of mucopolysaccharides in vesicle architecture and endothelial transport. *Journal of Cell Biology* **52**, 198–206.

SIMIONESCU, M. & SIMIONESCU, N. (1981). Hydrophilic pathways of capillary endothelium, a dynamic system. In *Water Transport across Epithelia, Alfred Benzon Symposium 15*, ed. USSING, H. H., BRINDSLEV, N., LASSEN, N. A. & STEN-KNUDSEN, O., pp. 228–247. Copenhagen: Munksgaard.

SMAJE, L. H. (1983). Permeability of salivary gland capillaries. In *Microcirculation of the Alimentary Tract*, ed. Koo, A., LAM, S. K. & SMAJE, L. H., pp. 167–177. Singapore: World Scientific Publishing Co.

TURNER, M. R., CLOUGH, G. & MICHEL, C. C. (1983). The effects of cationized ferritin and native ferritin upon filtration coefficients of single frog mesenteric capillaries. Evidence that proteins in the endothelial cell coat influence permeability. *Microvascular Research* **25**, 205–222.

WEIBEL, E. R. (1979). *Stereological Methods*, vol. I. *Practical Methods for Biological Morphometry*. London, New York, Toronto: Academic Press.

EXPLANATION OF PLATES

PLATE 1

Electron micrographs of the rabbit submandibular salivary gland perfused with cationized ferritin (pI > 10·5) and fixed by vascular perfusion with a modified Karnovsky's fixative. Upper micrograph shows control tissue in which the acinar (a) and duct (d) tissue is well formed and the capillary endothelium (c) coated by a relatively uniform layer of molecules of cationized ferritin. Lower micrograph shows a gland after 2 weeks duct ligation. The connective tissue (t) between the acini (a) appears fibrous and oedematous. The acini are ill formed and the capillary lumen (c) irregular. The layer of cationized ferritin appears uneven, and aggregates of cationized ferritin can be seen within the capillary lumen together with a red blood cell. Bars represent 2 μm.

PLATE 2

High-power electron micrographs of the capillary endothelium of vessels of the submandibular salivary gland, perfused with cationized ferritin (CF) prior to perfusion fixation. The vessel lumen in uppermost in each section and the well-defined fenestrae are indicated by ▲. *A*, section of a capillary from a control gland, perfused with CF at pI 8·5 which appears as an irregular layer at the cell surface. Molecules of CF can be seen in the fenestral regions. *B*, a capillary from a control gland perfused with CF (pI > 10·5). Note the more regular appearance of the layer of CF molecules, which appears to cover all the fenestrae. *C*, a capillary from a duct-ligated gland perfused with CF (pI > 10·5). The layer of CF molecules appears irregular and discontinuous. Bar represents 200 nm.

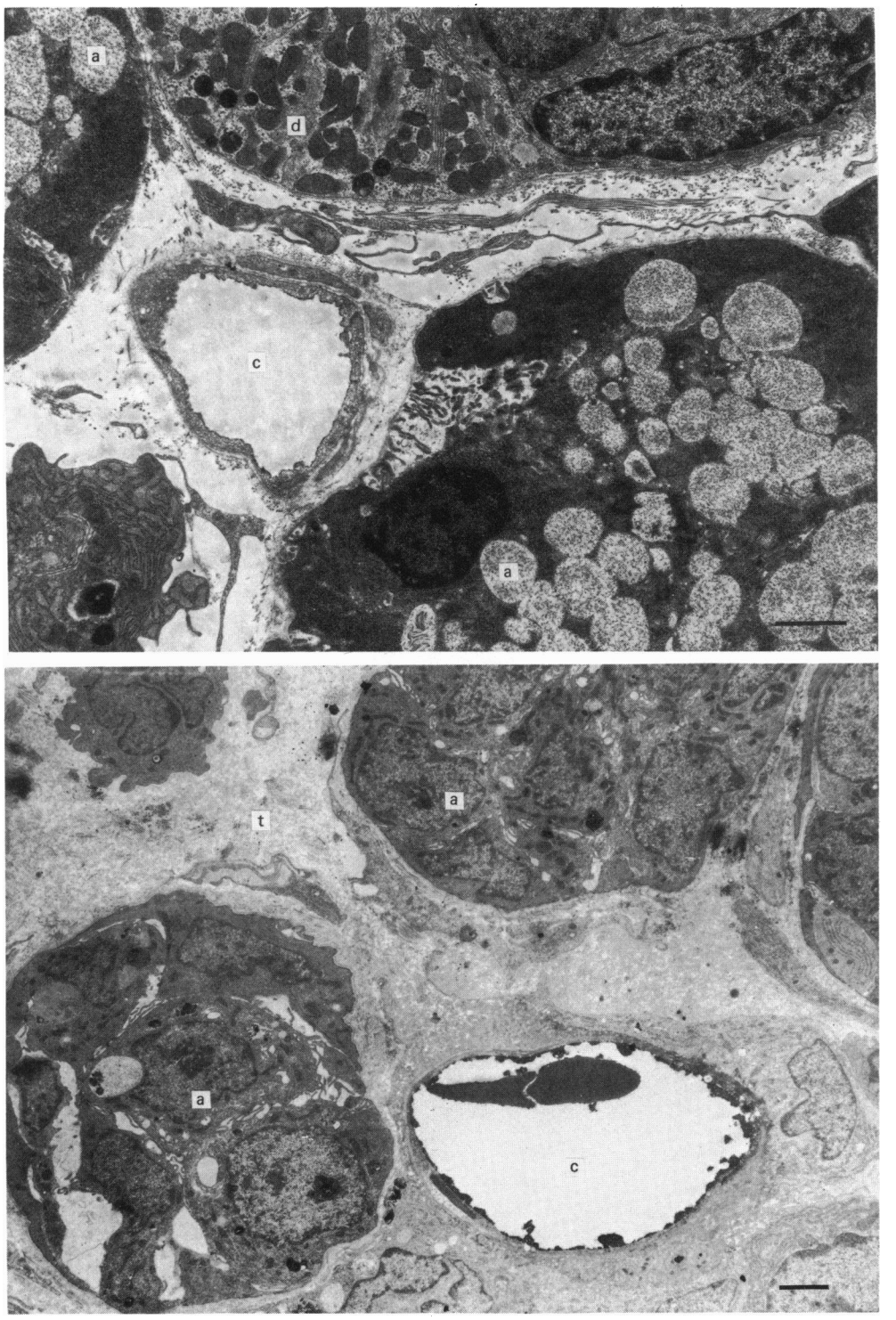

G. CLOUGH AND L. H. SMAJE

(*Facing p.* 456)

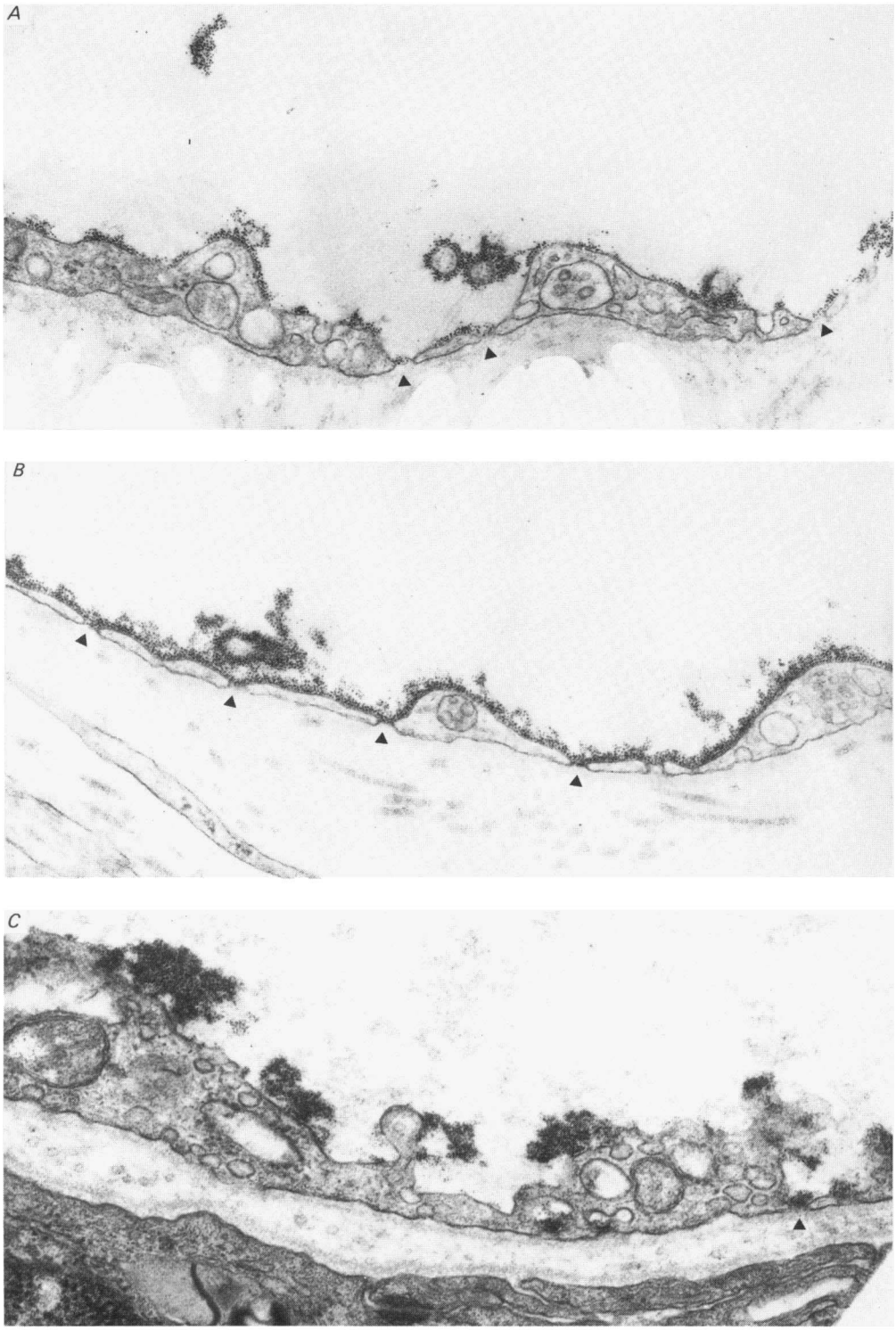
A
B
C